

MODIFICATION OF WEAKLY COMPRESSIBLE SMOOTHED PARTICLE HYDRODYNAMICS FOR PRESERVATION OF ANGULAR MOMENTUM IN SIMULATION OF IMPULSIVE WAVE PROBLEMS

B. ATAIE-ASHTIANI* and S. MANSOUR-REZAEI†

*Department of Civil Engineering,
Sharif University of Technology Tehran, Iran*

*ataie@sharif.edu

†sahebrezaei@gmail.com

*<http://sina.sharif.edu/~ataie>

Received 28 November 2008

Revised 17 October 2009

In this work, Weakly Compressible Smoothed Particle Hydrodynamics (WCSPH) is applied for numerical simulation of impulsive wave. Properties of linear and angular momentum in WCSPH formulation are studied. Kernel gradient of viscous term in momentum equation is corrected to ensure preservation of angular momentum. Corrected WCSPH method is used to simulate solitary Scott Russell wave and applied to simulate impulsive wave generated by two-dimensional under water landslide. In each of the test cases, results of corrected WCSPH are compared with experimental results. The results of the numerical simulations and experimental works are matched and a satisfactory agreement is observed. Furthermore, vorticity contours computed by the corrected WCSPH are compared with uncorrected WCSPH so that the effect of corrective term on preservation of angular momentum is illustrated. Numerical model is also applied for simulation of water entry of half buoyant circular cylinder into initially calm water. Comparison between experimental and computational results proves applicability of the WCSPH method for simulation of these kinds of problems.

Keywords: Angular momentum; weakly compressible SPH; impulsive waves; SPHysics.

*Corresponding author.

1. Introduction

Impulsive waves generated by landslides and slamming on horizontal cylindrical members of a jacket are examples of phenomena which cause damage on structures and endanger human life. Importance of wave generated by landslide has been a motivation for a large number of studies. There are some experimental works focused on the generated waves by rigid and deformable landslide [Heinrich, 1992; Grilli and Watts, 2005; Ataie-Ashtiani and Najafi-Jilani, 2008; Ataie-Ashtiani and Nikkhah, 2008]. Also, many numerical studies of landslide waves have been carried out by researchers. Jiang and LeBlond [1992] developed a fluid model to simulate water waves generated by deformable underwater landslides. Rzedkiewicz *et al.* [1997] simulated an under water landslide by introducing a two-phase description of sediment motion and using the volume of fluid (VOF) technique. Grilli and Watts [1999] simulated waves due to moving submerged body using a boundary element method. Ataie-Ashtiani and Malek Mohammadi [2007] evaluated the accuracy of empirical equations to estimate generated wave amplitude in the near field.

Recently, numerical methods that do not use a grid have been used in simulation and prediction of damage in these sophisticated hydrodynamic problems. One of these modern methods is Smoothed Particle Hydrodynamics (SPH). SPH was introduced for astrophysical applications [Lucy, 1977], but rapidly extended and used in engineering fields, including free surface flows and wave propagation [Monaghan, 1994; Monaghan and Kos, 1999]. Two different approaches have been used to extend SPH method to incompressible or nearly incompressible flows. In the first approach, called incompressible-SPH (I-SPH), the pressure is directly obtained by solving a Poisson equation of pressure that satisfies incompressibility [Shao and Lo, 2003]. In the second approach (WCSPH), unlike incompressible SPH method, real fluids are treated as compressible fluids with a sound speed which is much greater than the speed of bulk flow. Pressure of particles in this method is computed by a stiff equation of state [Monaghan, 1994]. WCSPH and I-SPH have been used by many researchers to investigate different hydrodynamic problems such as waves overtopping offshore platform deck, the breaking of a wave on a beach and bore in-a-box problem have been simulated using compressible SPH method [Dalrymple and Rogers, 2006]. Gómez-Gesteira and Dalrymple [2004] used three-dimensional SPH, and modeled the impact of single wave to the tall structure which was located in a region with vertical boundaries. Velocity and forces computed from numerical model were compared with laboratory measurement. The results showed that SPH method can successfully be used to simulate wave problems. Oger *et al.* [2006] proposed new formulation of the equation based on a SPH for spatially varying resolution (variable smoothing length). They simulated wedge water entry problem by using a new method to evaluate fluid pressure on solid boundaries. Ataie-Ashtiani and Shobeiry

[2008] presented an incompressible SPH (I-SPH) formulation to simulate impulsive waves generated by landslides. A new form of source term to the Poisson equation was employed, and the stability and accuracy of SPH method improved. Moreover, I-SPH method was used to simulate Dam-break flow, evolution of an elliptic water bubble, solitary wave breaking on a mild slope and run-up of non-breaking waves on steep slopes [Ataie-Ashtiani *et al.*, 2008]. Khayyer *et al.* [2008] corrected I-SPH method based on correction introduced by Bonet and Lok [1999], and achieved enhanced accuracy in modeling of the water surface during wave breaking and post-breaking.

A general model based on Weakly Compressible Smoothed Particles Hydrodynamics, “SPHysics”, was developed jointly by researchers at the Johns Hopkins University (USA), the University of Vigo (Spain), the University of Manchester (UK) and the University of Rome La Sapienza (Italy) to promote the development and use of SPH within the academic and industrial communities [SPHysics user guide, 2007]. SPHysics is provided for two and three-dimensional simulation of dam break in a box, dam break evolution over a wet bottom, waves generated by a paddle in a beach, tsunami generated by a sliding wedge and dam-break interaction with a structure [SPHysics user guide, 2007].

In SPHysics, Predictor-corrector and Verlet schemes are implemented. Also, two types of solid boundary conditions can be used for numerical simulation (Dynamic and Repulsive force boundary conditions). In addition, three different options for the simulation of viscosity are Artificial Viscosity, Laminar Viscosity, Sub-Particle Scale (SPS) Turbulence Model. SPHysics can simulate two- and three-dimensionally Dam break in a box, Dam break evolution over a wet bottom in a box, Waves generated by a paddle in a beach and Tsunami generated by a sliding Wedge. The selected following references are published by using SPHysics: [Dalrymple and Rogers, 2006; Gómez-Gesteira and Dalrymple, 2004; Crespo and *et al.*, 2007].

SPHysics model is used in this work and it is modified and improved in two aspects. First, shapes of boundary conditions in SPHysics are modified to simulate three problems about impulsive wave and impact on the water surface. Second, correction technique, which was introduced by Bonet and Lok [1999], is applied for the purpose that the accuracy of the SPH model is enhanced through the preservation of angular momentum. The corrected model is used to simulate solitary wave generated by Scott Russell, two-dimensional under water landslide and water entry of half buoyant circular cylinder into initially calm water.

Standard SPH formulations preserve linear momentum, but they do not usually preserve angular momentum, which plays a vital role in the case of violent free surface flows [Khayyer *et al.*, 2008; Bonet and Lok, 1999]. The main objective of this work is to improve precision of compressible SPH method through the preservation of angular momentum to simulate impulsive wave problems.

2. SPH Formulation for Compressible Fluid Flow

2.1. Basic SPH theory

SPH is an interpolation method which allows any function to be expressed in terms of its values at a set of disordered particles [Monaghan, 1992]. The fundamental principle is to approximate any function $A(\mathbf{r})$ by:

$$A(\mathbf{r}) = \int A(\mathbf{r}')w(\mathbf{r} - \mathbf{r}', h)d\mathbf{r}' \quad (1)$$

where h is called the smoothing length and $w(\mathbf{r} - \mathbf{r}', h)$ is the weighting function or kernel. For numerical work, the integral interpolant is approximated by summation interpolant [Monaghan, 1992]:

$$A(\mathbf{r}) = \sum_b m_b \frac{A_b}{\rho_b} w_{ab} \quad (2)$$

where the summation is over all the neighboring particles. ρ_b and m_b are density and mass, respectively, $w_{ab} = w(\mathbf{r}_a - \mathbf{r}_b, h)$ is weighting or kernel function which is similar to the delta function.

2.2. Governing equations

Governing equations of viscous fluid which are momentum and mass conservation equations are presented following [SPHysics user guide, 2007]:

$$\frac{D\mathbf{v}}{Dt} = -\frac{1}{\rho}\nabla P + \mathbf{g} + \Theta \quad (3)$$

$$\frac{1}{\rho}\frac{D\rho}{Dt} + \nabla \cdot \mathbf{v} = 0 \quad (4)$$

where ρ is density, \mathbf{v} is the velocity vector, P is the pressure, \mathbf{g} is acceleration due to gravity and Θ refers to the diffusion terms.

In conventional SPH notation of momentum and mass equations, artificial viscosity has been used [SPHysics user guide, 2007]:

$$\frac{d\mathbf{v}_a}{dt} = -\sum_b m_b \left(\frac{P_b}{\rho_b^2} + \frac{P_a}{\rho_a^2} + \Pi_{ab} \right) \nabla_a w_{ab} + \mathbf{g} \quad (5)$$

$$\frac{d\rho_a}{dt} = \sum_b m_b \mathbf{v}_{ab} \nabla_a w_{ab} \quad (6)$$

In the above equations, $\nabla_a \mathbf{w}_{ab}$ is gradient of the kernel with respect to the position of particle a . P_k and ρ_k are pressure and density of particle k (evaluate at a or b),

m_b is mass of particle b . Π_{ab} represents the effects of viscosity [SPHysics user guide, 2007]:

$$\Pi_{ab} = \begin{cases} \frac{-\alpha \bar{c}_{ab} \mu_{ab}}{\bar{\rho}_{ab}} & \mathbf{v}_{ab} \mathbf{r}_{ab} < 0 \\ 0 & \mathbf{v}_{ab} \mathbf{r}_{ab} > 0 \end{cases} \quad (7)$$

where α is an empirical coefficient, $\bar{c}_{ab} = (c_a + c_b)/2$, $\bar{\rho}_{ab} = (\rho_a + \rho_b)/2$ and $\mu_{ab} = \frac{h \mathbf{v}_{ab} \cdot \mathbf{r}_{ab}}{r_{ab}^2 + 0.01h^2}$; with $\mathbf{v}_{ab} = \mathbf{v}_a - \mathbf{v}_b$ and $\mathbf{r}_{ab} = \mathbf{r}_a - \mathbf{r}_b$; being \mathbf{r}_k and \mathbf{v}_k the position and velocity corresponding to particle k (a or b). α is free parameter.

In this work, we used quadratic kernel function from multifarious possible kernel in SPHysics. Ataie-Ashtiani and Jalali-Farahani [2007] displayed that in the simulation of impulsive waves, quadratic kernel is efficient and accurate:

$$w_{ab} = w(\mathbf{r}_a - \mathbf{r}_b, h) = \alpha_N (q^2/4 - q - 1), \quad 0 \leq q \leq 2 \quad (8)$$

where $q = r_{ij}/h$ and $\alpha_N = \frac{3}{2\pi h^2}$ for 2-D, $\alpha_N = \frac{15}{167\pi h^3}$ for 3-D, $r_{ij} = |\mathbf{r}_i - \mathbf{r}_j|$ and the coefficient h is the smoothing length.

2.3. Equation of state

The equation of state allows us to avoid an expensive resolution of an equation such as the Poisson's equation, but it inverts any incompressible fluid to the weakly compressible [SPHysics user guide, 2007]. The equation of state relates the pressure in the fluid to the local density:

$$P = B \left[\left(\frac{\rho}{\rho_0} \right)^\gamma - 1 \right] \quad (9)$$

where $\gamma = 7$, $B = C_0^2 \rho_0 / \gamma$ and C_0 is the speed of sound at reference density ($\rho_0 = 1000 \text{ kg/m}^3$). We cannot use physical sound speed in water because we should determine the speed of sound so low that time stepping remains reasonable. On the other hand, the speed of sound should be about ten times faster than the maximum fluid velocity in order to keep changes in fluid density less than 1% [Dalrymple and Rogers, 2006].

3. Viscosity

Artificial viscosity which originally was used in the equation of motion has a few advantages and disadvantages. First of all, in free surface problems, it plays the role of stabilizer in numerical scheme. Second, artificial viscosity prevents the particle from interpenetrating [Dalrymple and Rogers, 2006]. Then, it preserves both linear and angular momentum and has an acceptable manner in the case of rigid body rotations [Monaghan, 1992]. In contrast, the artificial viscosity has some disadvantages. It is a scalar viscosity which cannot take the flow directionally into account

[Khayyer *et al.*, 2008], and it causes strong dissipation and affects shears in the fluid [Dalrymple and Rogers, 2006]; thus, researchers prefer to simulate viscosity in a realistic manner.

One realistic expression of viscosity is Laminar viscosity [Morris *et al.*, 1997] and Sub-Particle Scale (SPS) technique to model turbulence. Researchers used SPS approach to modeling turbulence in some kind of particle methods such as MPS [Gotoh *et al.*, 2001] and Incompressible SPH [Lo and Shao, 2002]. Recently, Dalrymple and Rogers [2006] implemented this expression of viscosity in compressible SPH method. This facility is provided in SPPhysics code too, and we used Laminar Viscosity and Sub-Particle Scale (SPS) Turbulence in this paper. Implementing SPS approach in diffusion term of momentum equation [Eq. (3)] gives:

$$\frac{d\mathbf{V}}{dt} = -\frac{1}{\rho}\nabla P + \mathbf{g} + \nu_0\nabla^2\mathbf{V} + \frac{1}{\rho}\nabla\tau \quad (10)$$

where $\nu_0\nabla^2\mathbf{V}$ represents laminar viscosity term, and τ represents SPS stress tensor, which was modeled by eddy viscosity assumption very often [SPPhysics user guide, 2007]. Dalrymple and Rogers [2006] wrote momentum equation [Eq. (10)] in SPH notation using laminar viscosity and SPS:

$$\begin{aligned} \frac{d\mathbf{V}_a}{dt} = & -\sum_b m_b \left(\frac{P_b}{\rho_b^2} + \frac{P_a}{\rho_a^2} \right) \nabla_a w_{ab} + \mathbf{g} + \sum_b m_b \left(\frac{4\mathbf{v}_0\mathbf{r}_{ab}\mathbf{v}_{ab}}{|\mathbf{r}_{ab}|^2(\rho_a + \rho_b)} \right) \nabla_a w_{ab} \\ & + \sum_b m_b \left(\frac{\tau_b}{\rho_b^2} + \frac{\tau_a}{\rho_a^2} \right) \nabla_a w_{ab} \end{aligned} \quad (11)$$

where ν_0 is the kinetic viscosity of laminar flow (10^{-6} m²/s).

4. Preservation of Angular Momentum

In the absence of external forces, the motion of particles must be such that the total linear and angular momentum is preserved. In this section, we explain that standard SPH formulations inherently preserve linear momentum, but generally cannot preserve angular momentum.

In the absence of external forces, combination of time derivation of total linear momentum with Newton's second law gives the condition for the preservation of linear momentum [Bonet and Lok, 1999; Khayyer *et al.*, 2008]:

$$\sum_{i=1}^N A_i = 0 \quad (12)$$

where A_i denotes the total internal force acting on particle i , and N is total number of particles.

Interaction forces between pairs of particles have two components; one part is related to the pressure gradient and another part is related to the viscous term.

Khayyer *et al.* [2008] wrote kernel gradient as a function of r_{ij} . They showed that interaction forces between pairs of particles (due to pressure and viscosity) are exactly equal and opposite. This means that their influences are vanished, and linear momentum is preserved by SPH formulations.

Similarly, in the absence of external forces, combination of time derivation of total angular momentum with equilibrium equation gives the condition for the preservation of angular momentum. Rate of change of total angular momentum will be zero (angular momentum will be preserved), provided that internal force between pairs of particles are collinear with vector of r_{ij} [Bonet and Lok, 1999; Khayyer *et al.*, 2008]. Because of the fact that pressure stress tensor is isotropic, internal force due to pressure term is collinear with vector of r_{ij} [Khayyer *et al.*, 2008]. Therefore, angular momentum, which is produced by pressure force, equals zero precisely. The same is not true about internal force due to viscosity (when we use one realistic expression of viscosity) because viscous stress tensor is anisotropic, and internal viscous force which is not collinear with r_{ij} produces a momentum.

To sum up, pressure gradient in momentum equation preserves both linear and angular momentums, but viscosity term, which is described by laminar viscosity and Sub-Particle Scale (SPS) Turbulence, cannot preserve angular momentum despite the fact that it is a good expression of realistic viscosity.

4.1. Corrective term

In previous sections, we mentioned that artificial viscosity has considerable disadvantages. Thus, applications of realistic viscosity such as laminar viscosity and Sub-Particle Scale (SPS) Turbulence are increasing. Also, we explain that viscous term in momentum equation cannot preserve angular momentum. As a result, it seems that preservation of angular momentum will help to obtain more accurate results.

Researchers have used a number of correction techniques in the hope that accuracy of the SPH method enhances through the preservation of angular momentum. Some researchers correct kernel functions, while others correct gradients of kernel functions. In this work, similar to the Khayyer *et al.* [2008], we apply correction of kernel gradients (L_i) introduced by Bonet and Lok [1999] due to its simplicity:

$$\overline{\nabla_i w_{ij}} = L_i \nabla_i w_{ij}$$

$$L_i = \left(\sum \frac{m_j}{\rho_j} \nabla_i w_{ij} \otimes (\mathbf{r}_j - \mathbf{r}_i) \right)^{-1} \quad (13)$$

where $\overline{\nabla_i w_{ij}}$ is the corrected kernel gradient.

On the ground that pressure gradient in momentum equation preserves both linear and angular momentum, this correction is only used during the calculation of viscous term in momentum equation. Using this correction technique will guarantee that the gradient of any linear velocity is properly evaluated. In addition, both

pressure gradient term and viscosity term preserve angular momentum [Bonet and Lok, 1999].

The correction technique to preserve angular momentum may violate the anti-symmetric form of equations leading to a violation of Newton's third law [Khayyer and Gotoh, 2008] because corrective function calculated for a target particle a would not be necessarily equal to that calculated for its neighboring particle b . However, using correction terms guarantees the preservation of angular momentum and exact calculation of the gradient of any linear velocity field. Recent publications [Khayyer *et al.*, 2008; Bonet and Lok, 1999] showed successful application of this correction method in the simulation of highly non-linear physical processes.

4.2. Validation of corrected model

Simulating the evolution of an elliptic water bubble is carried out to illustrate development of model through preservation of angular momentum. Initial configuration of particles is a 1 unit circle. The initial particle spacing $L_0 = 0.05$ m (1,316 particles), initial density $\rho = 1,000$ kg/m³ and the constant time step $\Delta t = 6.5 \times 10^{-7}$ s were employed in the computations. The drop moves with initially velocity field as $(-100x, -100y)$ m/s. Initial position and initial velocity of particles are shown in Fig. 1. During the simulation due to the absence of external forces total linear and angular momentum should be preserved. In Fig. 2 variations of total Y -direction linear and angular momentum during the evolution are illustrated. As shown, correcting kernel gradient in viscous term of momentum equation, lead to preserve angular

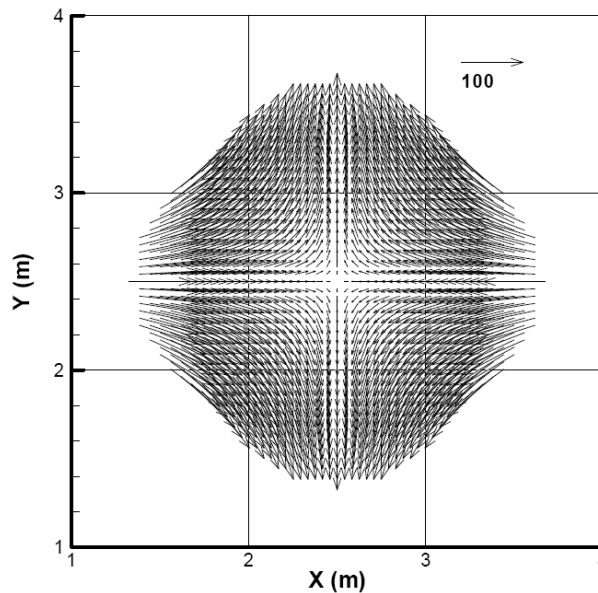


Fig. 1. Initial position and initial velocity of particles in the water bubble flow simulation.

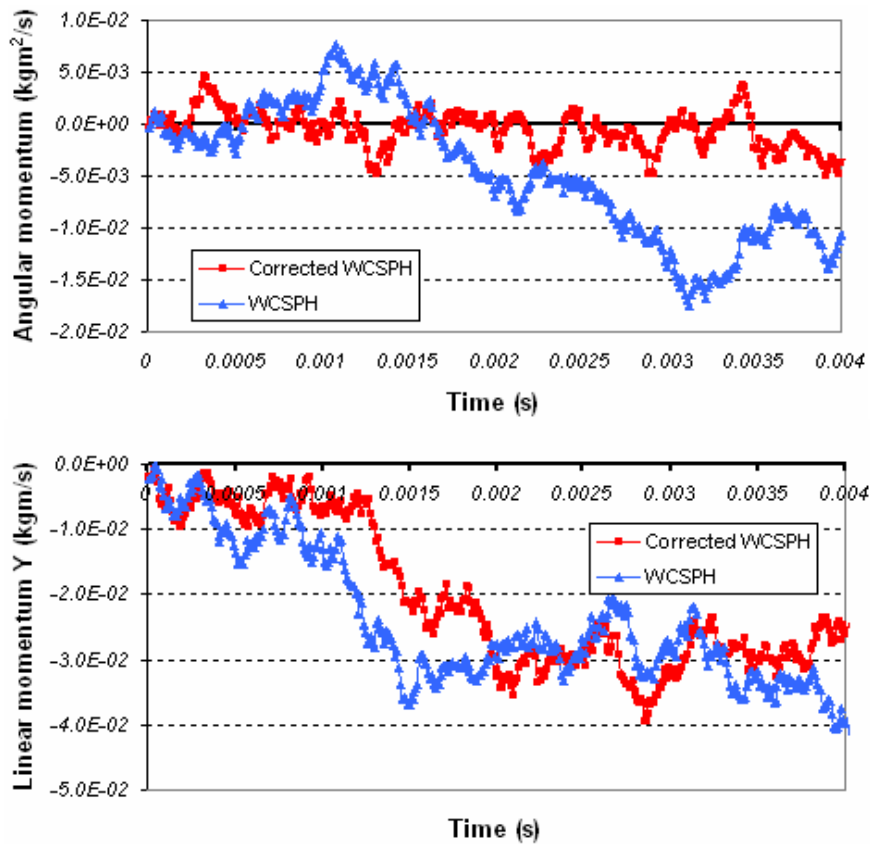


Fig. 2. Total angular momentum (Top) and total Y -direction linear momentum (Bottom) in corrected WCSPH and WCSPH- an elliptical water drop simulation.

momentum. However, this correction does not change variation of total Y -direction linear momentum. Although exact preservation of linear momentum has been expected in Fig. 2, violation of linear momentum can be seen in both the corrected and uncorrected results. It appears that compressibility effect and numerical error generate this kind of behavior. Time of operation in model using correction method was 865 seconds, and time of operation in model not using correction method was 688 seconds.

The evolution of an elliptic water bubble can also be solved in an analytical way [Monaghan, 1994]. The theoretical values of semi-major axis of the drop at different times and the values computed by WCSPH method and the corrected WCSPH method are shown in Table 1. The results show that preservation of angular momentum does not influence water surface. Comparisons of numerical results with analytical solutions are made until 0.004 s because some compressibility instability had been generating. This instability has an effect on both corrected and uncorrected model.

Table 1. Theoretical and computational values of semi-major axis.

Time (s)	WCSPH	Corrected WCSPH	Theory
0.001	1.106	1.106	1.104
0.002	1.222	1.222	1.218
0.003	1.344	1.344	1.338
0.004	1.472	1.472	1.464

5. Test Cases

In this section, the results of numerical simulation for three examples of impulsive waves are given. In each of the test cases, results of corrected WCSPH are compared with experimental data. Also, in the simulation of Scott Russell wave generator and under water rigid landslide, vorticity contours of corrected and uncorrected method are compared. Comparisons show that preservation of angular momentum affects shape and intensity of vorticity.

In numerical simulations, Prediction-correction algorithm, Dalrymple boundary condition and Shephard filtering techniques are employed. These techniques are described in details in following papers [Monaghan, 1989; Crespo *et al.*, 2007; Dalrymple and Knio, 2000; SPHysics user guide, 2007].

5.1. *Scott Russell wave generator*

Researchers frequently use the Scott Russell wave generator to simulate falling avalanche in dam reservoirs and to assess the behavior of waves generated by landslides near slopes. Monaghan and Kos [2000] evaluated this problem both experimentally and numerically [using SPH method]. Besides, Ataie-Ashtiani and Shobeyri [2008] numerically simulated experimental data of Monaghan and Kos by employing a new form of source term to the Poisson equation.

In this section, solitary waves generated by a heavy box falling vertically into the water are considered. Also, the effect of preservation of angular momentum in the generation of impulsive waves and its influence to obtain more accurate result are evaluated. Boundary conditions in SPHysics code, including the shape of tank and sliding wedge are changed according to the Monaghan and Kos [2000] experiments configuration. The experiment involved a weighted box (0.3 m \times 0.4 m) dropping vertically into a wave tank while still water depth is 0.21 m. The initial condition of the problem is shown in Fig. 3. It should be noted that the horizontal length of the numerical tank is assumed to be 2 m, which is much shorter than the experimental tank (9 m). However, numerical results show that this assumption does not affected results even in the maximum time of simulation. The bottom of the box was initially placed 0.5 cm below the water surface in the experiment to avoid splashing. Vertical

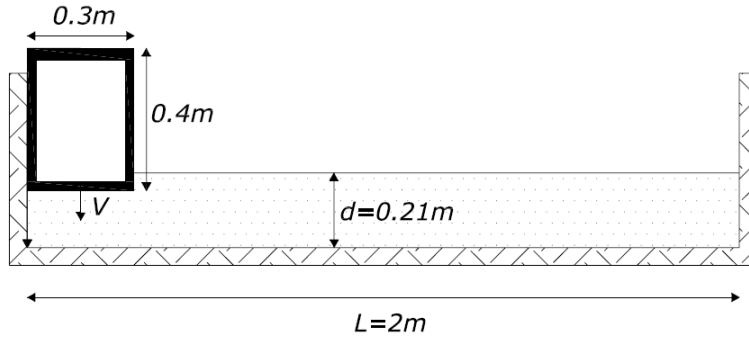


Fig. 3. Initial conditions of Scott Russell wave generator test case.

velocity of the box is computed by [Monaghan and Kos, 2000]:

$$\frac{V}{\sqrt{gD}} = 1.03 \frac{Y}{D} \left(1 - \frac{Y}{D}\right)^{0.5} \quad (14)$$

where D is the depth of the water, Y is the height of the bottom of the box above the bottom of the tank at time t , g is the acceleration of gravity and V is the falling vertical velocity of the box at time t . Analytical shape of solitary wave generated by falling box calculated by [Lo and Shao, 2002]:

$$H(x, t) = a \times \sec h^2 \left[\sqrt{\frac{3a}{4d^3}} (x - ct) \right] \quad (15)$$

where H is the water surface elevation, a is wave amplitude, d is water depth and $c = \sqrt{g(d+a)}$ is solitary wave velocity.

In Fig. 4 particles configurations display solitary wave formation when WCSPH method preserved angular momentum. In numerical simulation, initial particles space and speed of sound were 0.015 m and 16 m/s respectively. Figure 5 illustrates that analytical profile of solitary wave [Eq. (15)] is in good agreement with numerical result.

Some characteristic lengths of the solitary wave are shown in Fig. 6. In Table 2, results of corrected WCSPH and uncorrected SPH at $t = 0.285$, are compared with experimental values and previous works. Similar to validation test, it seems that correcting SPHysics to preserve angular momentum does not have considerable effect on water surface profile in impulsive wave generated by Scott Russell. Note that parameter Y at $t = 0.285$ s was about 0.094 m in experiment, while according Eq. (14), Y was assumed 0.085 m in simulation. Figures 7 and 8 judge against vorticity contour in corrected and uncorrected method at $t = 0.42$ s and $t = 0.7$ s, respectively. Vorticity contour computed by corrected model in Figs. 7 and 8 seems more localized. Also, water surface profile computed by corrected model in Fig. 7 is smoother than that computed by uncorrected model. These pictures show that preservation of angular momentum changes vorticity patterns slightly in fluid motion.

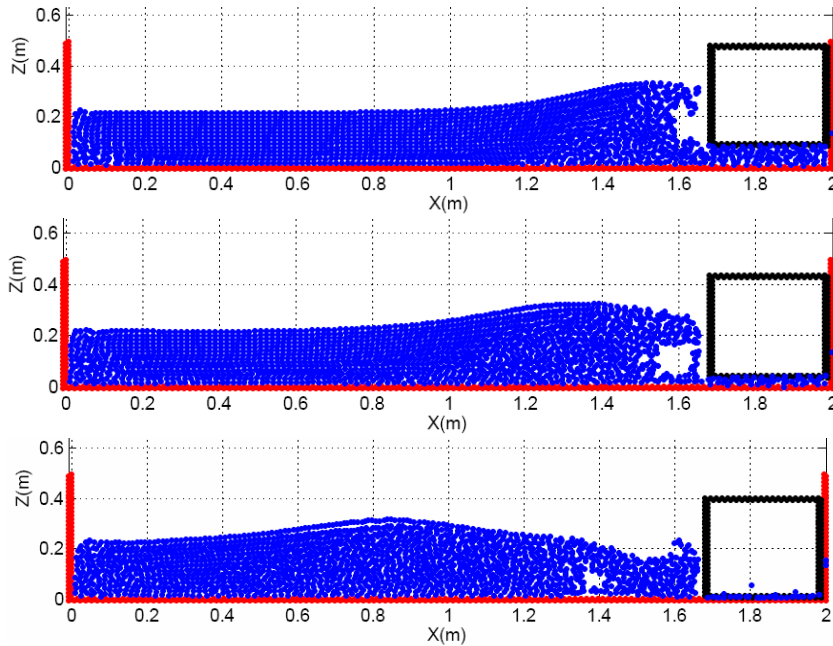


Fig. 4. Particles configuration in Scott Russell wave generator computed by corrected WCSPH at $t = 0.285$, $t = 0.42$ and $t = 0.7$ s, respectively, $l_0 = 0.015$ cm.

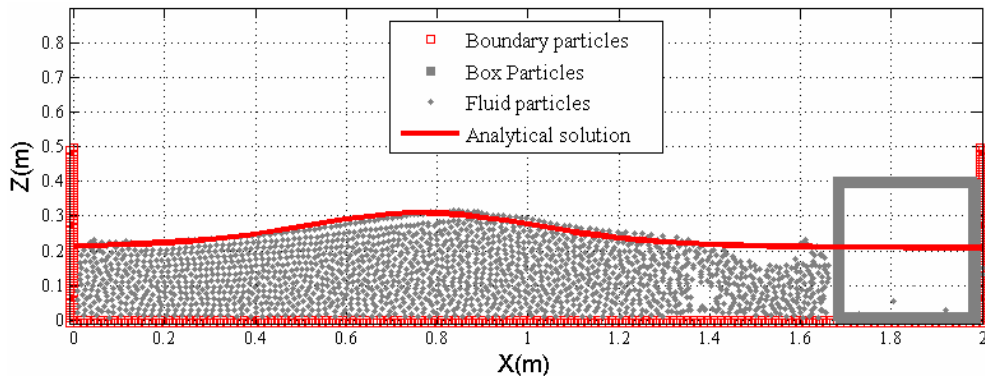


Fig. 5. Comparison between analytical solution and numerical result in Scott Russell problem, $t = 0.7$ s, $l_0 = 0.015$ cm.

5.2. Under water rigid landslide

In this section, the corrected WCSPH is used to simulate wave generated by two-dimensional under water landslide, based on a laboratory experiment performed by Heinrich [1992]. The experiment includes (Fig. 9) freely slide down rectangular wedge ($0.5 \text{ m} \times 0.5 \text{ m}$) on the plane which is inclined 45° to the horizontal. The water depth in the tank is 1 m, and top of the wedge is initially 1 cm below the water surface. The flat length of tank in computational domain is 3 m, and particles size

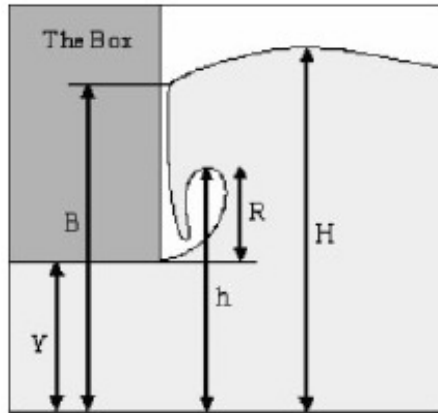


Fig. 6. Definitions of the parameters of Scott Russell wave generator problem [Monaghan and Kos, 2000].

Table 2. Comparison between the length h , H , B , R computed by present method, I-SPH [Ataie-Ashtiani and Shobeyri, 2008], SPH [Monaghan and Kos, 2000] and experimental result.

Initial particle spacing l_0 (m)	Method	H (m)	R (m)	h (m)	B (m)
0.015	Present work*	0.3318	0.1551	0.237	0.3115
0.015	Uncorrected algorithm*	0.3303	0.1621	0.2465	0.3073
0.015	Present work**	0.3346	0.1451	0.2269	0.2932
0.015	Uncorrected algorithm**	0.3327	0.1347	0.2191	0.2934
0.015	I-SPH	0.329	0.13	0.218	0.255
0.01	I-SPH	0.3301	0.146	0.234	0.268
0.0105	SPH	0.308	0.075	0.169	0.273
0.007	SPH	0.308	0.099	0.193	0.261
0.00525	SPH	0.309	0.109	0.203	0.273
0.0042	SPH	0.3086	0.114	0.208	0.272
—	Experimental	0.333 ± 0.01	0.1333 ± 0.02	0.2273 ± 0.02	0.303 ± 0.02

*speed of sound: 16 m/s

**speed of sound: 13 m/s

is 0.02 m. The position of the wedge in each time step is estimated by computing vertical velocity of wedge by [Grilli and Watts, 1999]:

$$\begin{cases} u(t) = c_1 \tanh(c_2 t) & t \leq 0.4 \text{ s} \\ t(t) = 0.6 & t > 0.4 \text{ s} \end{cases} \quad (16)$$

where c_1 and c_2 are constant values that in our computations are 86 and 0.0175, respectively. In Fig. 10, particle configuration due to sliding of rigid wedge at $t = 0.5$ s and $t = 1$ s is presented, and results of corrected WCSPH and experimental wave profile are compared. Inherent limitation of WCSPH, entrance of air at the location of impact and some difficulties for using finer particles are main complexities to obtain exact agreement. The maximum and minimum elevation of water at $t = 1$ s are 1.075 m and 0.764 m, respectively. In Figs. 11(a) and 11(b) the velocity field of

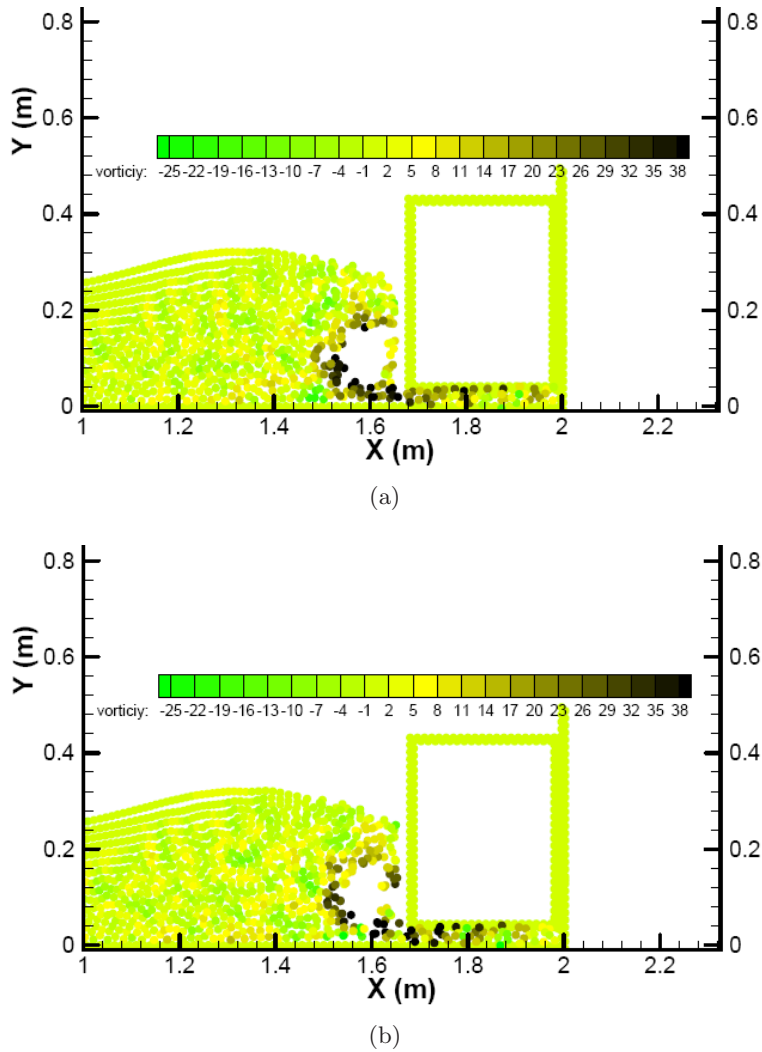


Fig. 7. Vorticity contour computed by corrected (a) and uncorrected (b) WCSPH at $t = 0.42$ s for the Scott Russell wave generator test case.

problem is presented at $t = 1$ s and $t = 0.5$ s. Figure 11(a) depicts impact of water jet to the top of wedge while wedge is sliding along slope. Figure 11(b) shows vortex generated above the sliding wedge at $t = 1$ s. In this figure, particles of wedge have no velocity because they reach the bottom of the tank. Figure 12 contrasts vorticity contour by corrected and uncorrected algorithm. As shown in Fig. 12(a), vorticity by corrected algorithm is more localized rather than vorticity in uncorrected WCSPH, which is shown in Fig. 12(b). Furthermore, the tail of vortex above the wedge in Fig. 12(a) represents preservation of the angular momentum and shedding of them. Although differences between water surface profile of corrected and uncorrected WCSPH are not significant, the results of corrected WCSPH are slightly

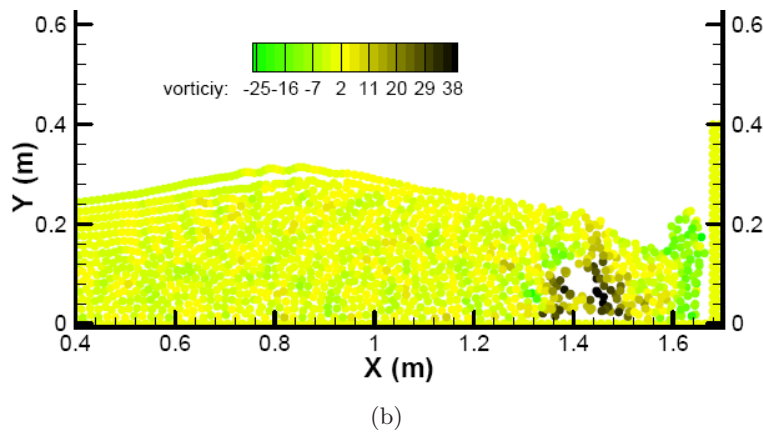
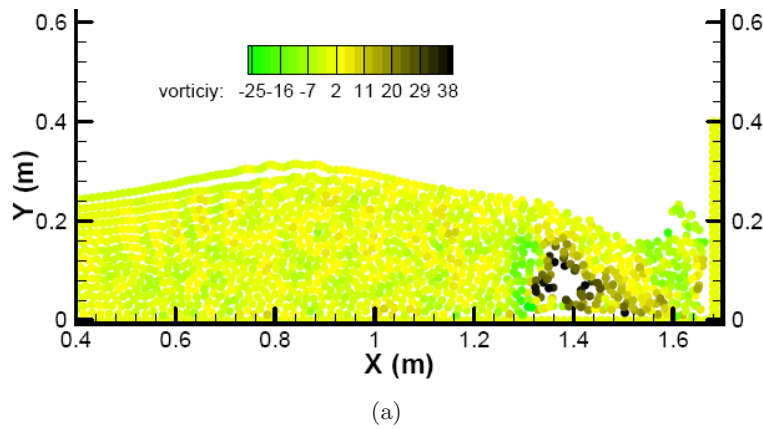


Fig. 8. Vorticity contour computed by corrected (a) and uncorrected (b) WCSPH at $t = 0.7$ s for the Scott Russell wave generator test case.

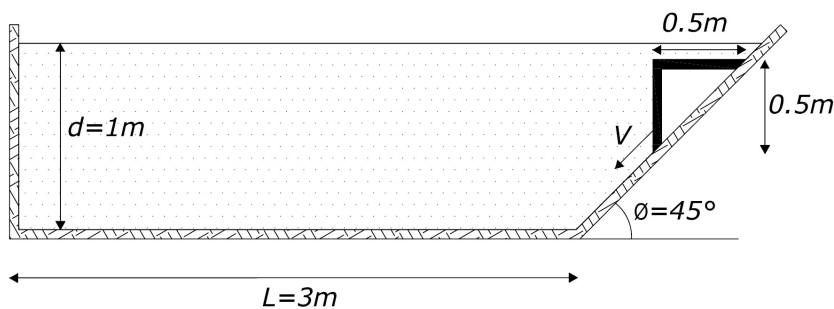


Fig. 9. Initial conditions of the under water rigid wedge sliding.

closer to the experimental measurements in comparison with uncorrected WCSPH (Fig. 13).

Lee *et al.* [2008] applied WCSPH and I-SPH for simulation of dam break, cavity flow and dam break on downstream wetbeds. They showed the velocity and

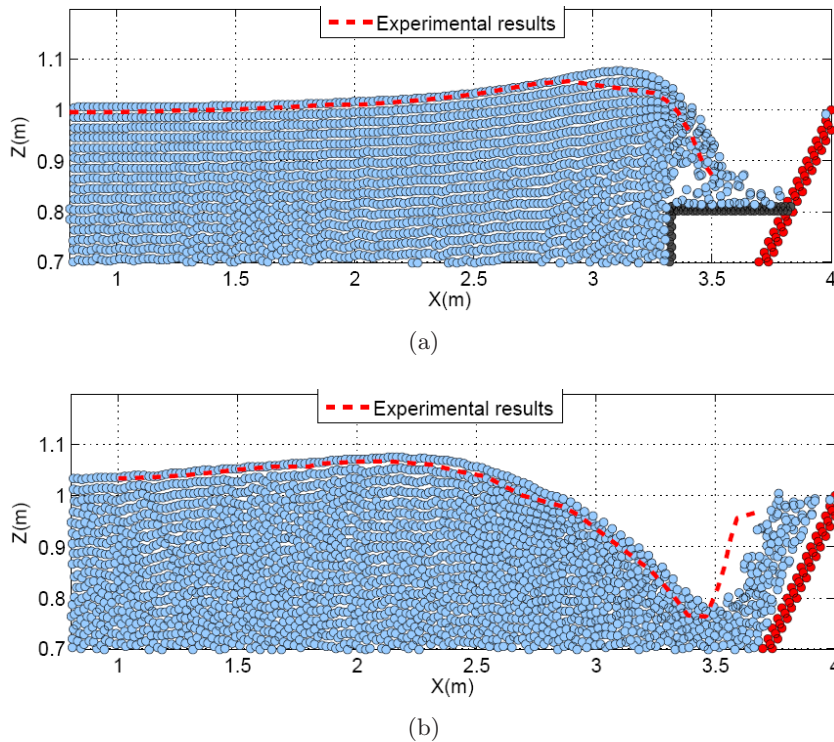
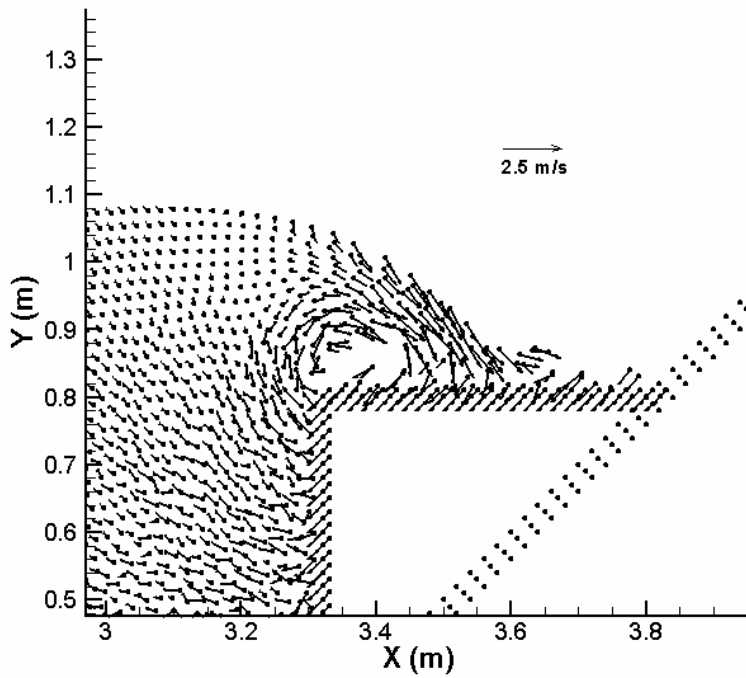


Fig. 10. Comparison between experimental and the simulating wave profile for under water rigid landslide at (a) $t = 0.5$ s and (b) $t = 1$ s.

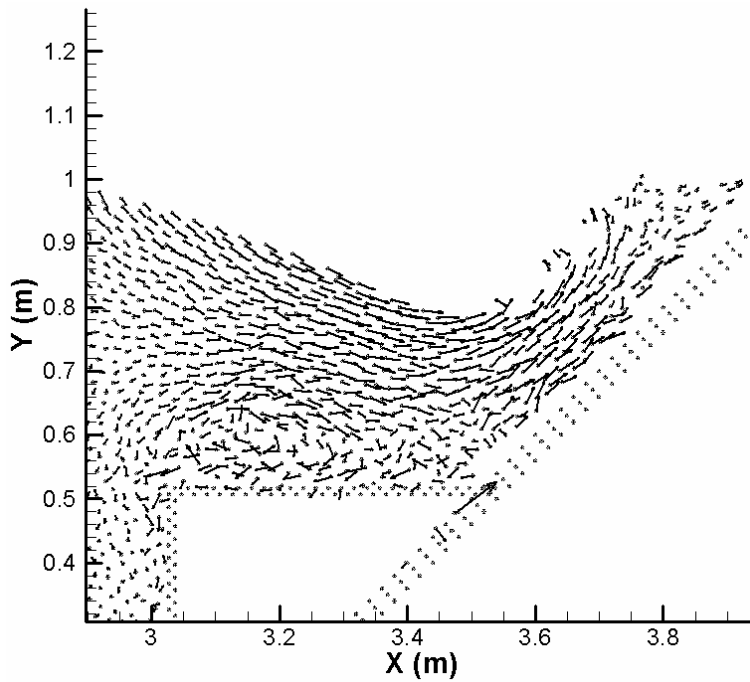
pressure in I-SPH is more reliable than WCSPH. Similarly, comparison between the experimental and numerical results of corrected WCSPH and I-SPH is shown in Fig. 14. It can be seen that ISPH water surface profiles are closer to experiment than the corrected WCSPH.

5.3. *Entry of a circular cylinder in water tank*

The slamming loads are concerned in offshore operation and motivated researchers for experimental and numerical studies. As a case in point, Greenhow and Lin [1983] performed some two-dimensional experiments and considered intersection of free surface and a moving body. In one of their experiments “half buoyant” cylinder dropped freely into initially calm water. Half buoyant means that the cylinder’s weight equals one half of the buoyancy force on a totally submerged cylinder [Sun and Faltinsen, 2006]. In their experiment, the diameter of cylinder is 0.11 m, and the falling distance is 0.445 m, which is measured from the bottom of cylinder. Cylinder impact water surface at $t = 0.301$ s while entry speed is 2.955 ms^{-1} . Figure 15 shows experimental depth of penetration of half buoyant cylinder into the water [Sun and Faltinsen, 2006].

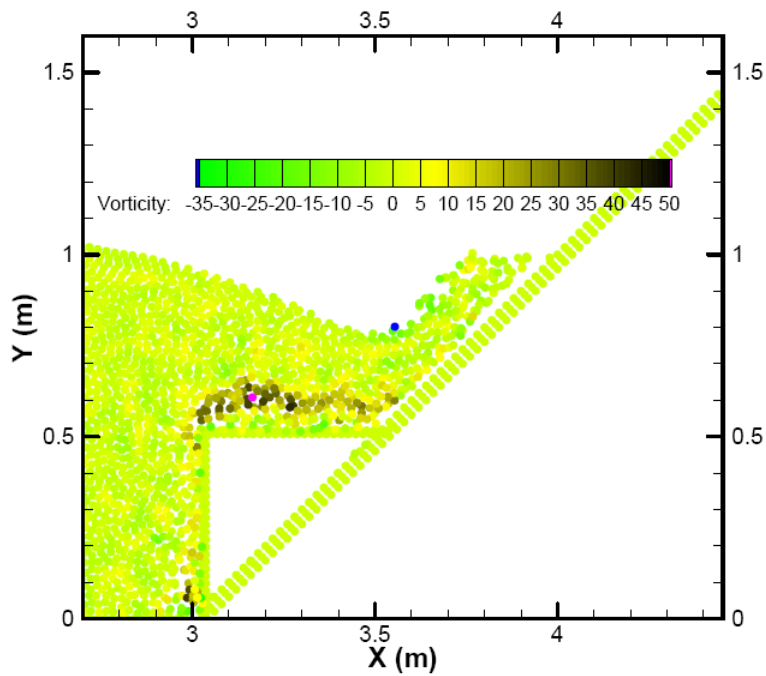


(a)

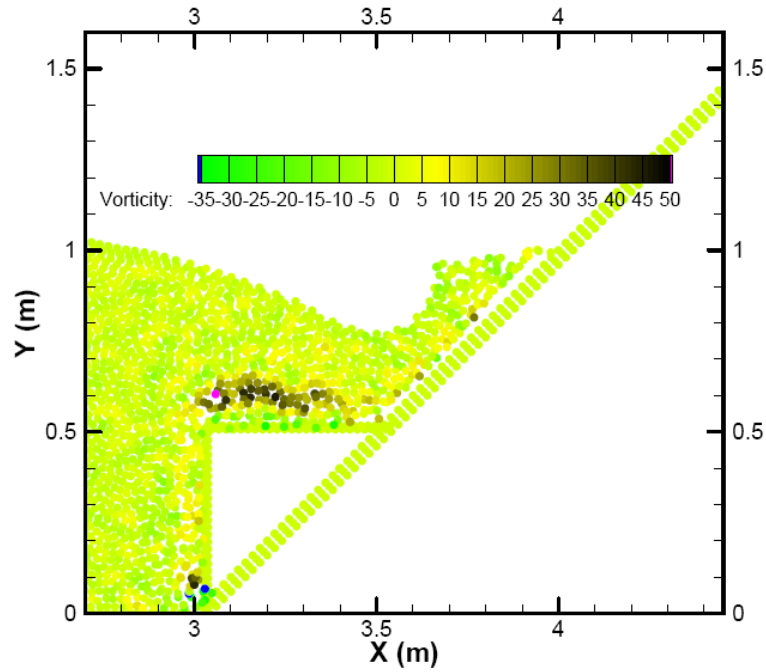


(b)

Fig. 11. Velocity field computed by corrected WCSPH at (a) $t = 0.5$ s and (b) $t = 1$ s for under water rigid landslide.



(a)



(b)

Fig. 12. Vorticity contour in under water rigid landslide computed by corrected (a) and uncorrected (b) WCSPPH at $t = 1$ s.

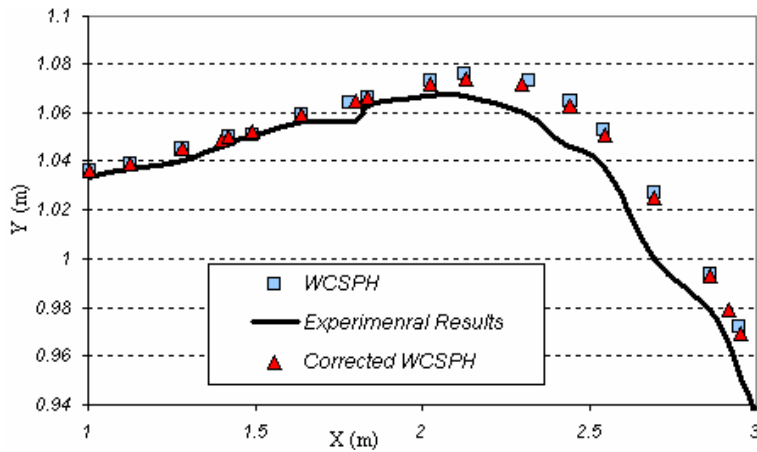


Fig. 13. Under water rigid landslide computed by corrected WCSPH are compared with WCSPH and Experimental results.

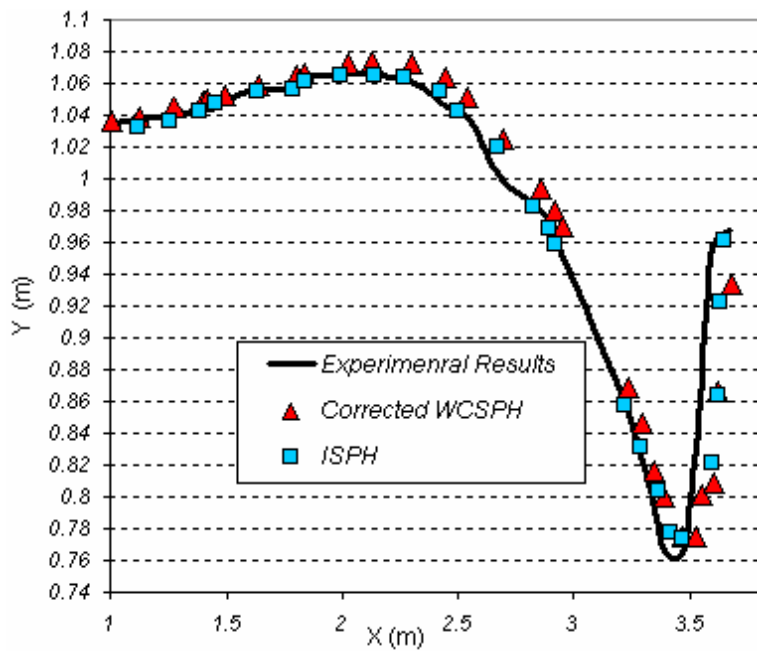


Fig. 14. Comparison between I-SPH (Ataie-Ashtiani and Shobeyri, 2008), Corrected WCSPH and experimental water surface elevations at $t = 1$ s for under water rigid landslide.

In this section, Greenhow and Lin [1983] laboratory experiments is modeled with corrected WCSPH. Penetration depth of cylinder in numerical simulation is recorded (Fig. 15). Also, we assume that changing between two points in Fig. 15 is linear. The computational domain is a box with 1 m length and 0.5 m height. The initial depth of the calm water is assumed to be 0.31 m. The particles sizes are 0.005 m.

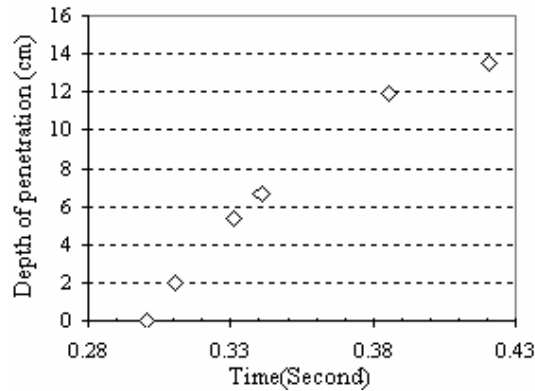


Fig. 15. Depth of penetration of half buoyant circular cylinder, cylinder impact water surface at $t = 0.301$ s.

The dimensions of tank are chosen so large that the height of the water near the wall even in maximum time of simulation does not change.

In Fig. 16, particle configurations due to impact of circular cylinder on the water surface are compared with experimental photos [Greenhow and Lin, 1983] at $t = 0.305$, $t = 0.320$, $t = 0.330$ and $t = 0.385$. Results show that the numerically predicted free surfaces are in moderately good agreement with experiment. In Fig. 17, the effect of decreasing the particle size is illustrated at $t = 0.385$. The differences between the results corresponding to $d = 0.004$ m and $d = 0.005$ m is less than that seen between the results with $d = 0.005$ m and $d = 0.01$ m. Also, in this figure free surface profile simulated by Boundary Element Method (BEM) [Hui, 2007] is shown. Although WCSPH results converge to the experimental data and BEM results by employing more particles, there are some differences between WCSPH and BEM results. We believe that main problem is about boundary conditions because after water separation from body surface or before impact to the water surface, boundary particles force to neighbor fluid particles, which leads to unphysical behavior.

In Fig. 16(d), numerical free surface profile seems to have a little roughness. We believe that small number of experimental data (Fig. 15) causes unsmooth motion of cylinder in numerical simulation and eventually this happens. It should be noted that it is necessary to use equation of motion or experimental data of moving objects because in SPHysics, motion of object is not calculated according to the governing laws of motion.

6. Conclusion

In this paper, corrected weakly compressible smoothed particles hydrodynamics (WCSPH) was used for numerical simulation of impulsive waves. Laminar viscosity and Sub-Particle Scale turbulence were employed to simulate viscosity in

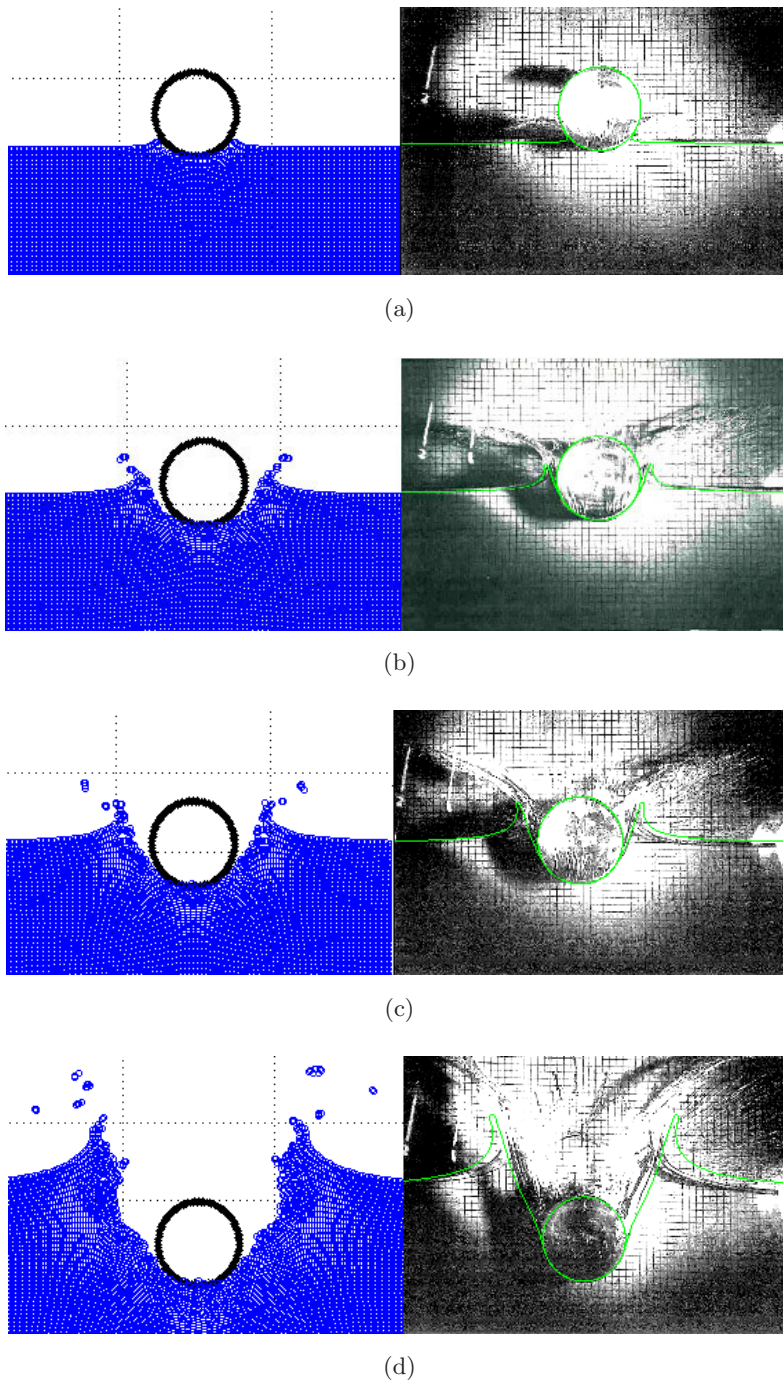


Fig. 16. Comparison of free surface profile in corrected WCSPH with experimental photos [Greenhow and Lin, 1983] at (a) $t = 0.305$, (b) $t = 0.320$, (c) $t = 0.330$ and (d) $t = 0.385$. Green lines in experimental photos are drawn by Sun and Faltinsen [2006] in order to compare with BEM.

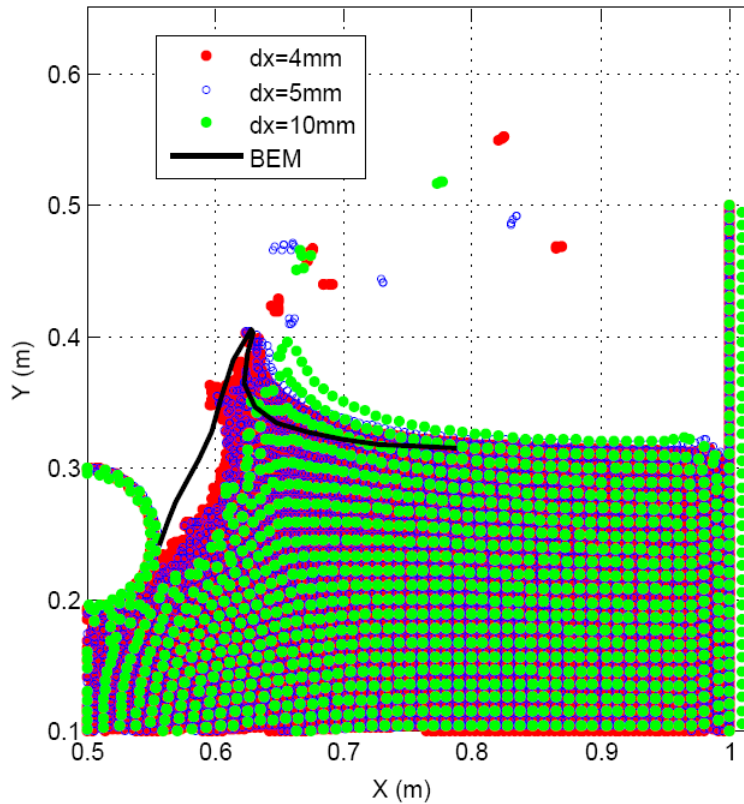


Fig. 17. Convergence of numerical results by decreasing the particle size (employing more computational particles) at $t = 0.385$ s.

impulsive wave problems. Kernel gradient of viscous term in momentum equation was corrected in order to preserve angular momentum and improve precision of WCSPH method. Corrected method was used to simulate Scott Russell wave, under water rigid wedge sliding along an inclined surface, and water entry of half buoyant circular cylinder. The computational WCSPH results were in moderately good agreement with the experimental data, which are showing the ability of the meshless methods to successfully simulate such kind of complex problems. In simulation of impulsive waves, the corrective term changed vorticity patterns somewhat and caused smoother water surface; however, this correction technique had no significant role to change water surface elevation.

Recently, SPHysics has been used successfully for a wide range of free surface flow problems. Several papers have been published using SPHysics which cover sediment transport, water overtopping, fluid-solid interaction, and tsunamis. However, improving the model to eliminate some limitations of the code would enable users to simulate more problems as well as to reach more precise results. For example, it would be useful to implement periodic boundary conditions in 2D simulation, or improving the model such that motion of an object can be calculated according to the

governing laws of motion. Also, improving SPHysics to be able to exactly conserve linear and angular momentum (in case of application of a realistic strain-based viscosity or consideration of turbulence modeling) should be a concern for future work.

References

- Ataie-Ashtiani, B. & Malek-Mohammadi, S. [2007] “Near field amplitude of sub-aerial landslide generated waves in dam reservoirs,” *Dam Engineering* **17**(4), 197–222.
- Ataie-Ashtiani, B. & Jalali-Farahani, R. [2007] “Improvement and application of I-SPH method in the simulation of impulsive waves,” in *Proc. Int. Conf. Violent Flows*, Fukuoka, Japan, pp. 116–121.
- Ataie-Ashtiani, B. & Najafi-Jilani, A. [2008] “Laboratory investigations on impulsive waves caused by underwater landslide,” *Coastal Engineering* **55**(4), 989–1004.
- Ataie-Ashtiani, B. & Nik-khah, A. [2008] “Impulsive waves caused by subaerial landslides,” *Environmental Fluid Mechanics* **8**(3), 263–280.
- Ataie-Ashtiani, B. & Shobeiry, G. [2008] “Numerical simulation of landslide impulsive waves by modified smooth particle hydrodynamics,” *Int. J. Numerical Methods in Fluids* **56**(2), 209–232.
- Ataie-Ashtiani, B., Shobeiry, G. & Farhadi, L. [2008] “Modified Incompressible SPH method for simulating free surface problems,” *Fluid Dynamics Research* **40**(9), 637–661.
- Bonet, J. & Lok, T. S. [1999] “Variational and momentum preservation aspects of smooth particle hydrodynamic formulation,” *Comput. Methods Appl. Mech. Eng.* **180**, 97–115.
- Crespo, A. J. C., Gómez-Gesteira, M. & Dalrymple, R. A. [2007] “Boundary conditions generated by dynamic particles in SPH methods,” *Computers, Materials & Continua* **5**(3), 173–184.
- Dalrymple, R. A. & Knio, O. [2000] “SPH modeling of water waves,” in *Proc. Coastal Dynamics*, Lund.
- Dalrymple, R. A. & Rogers, B. D. [2006] “Numerical modeling of water waves with the SPH method,” *Coastal Engineering* **53**, 141–147.
- Gómez-Gesteira, M. & Dalrymple, R. [2004] “Using a 3D SPH method for wave impact on a tall structure,” *Journal of Waterway, Port, Coastal and Ocean Engineering* **130**(2), 63–69.
- Greenhow, M. & Lin, W. M. [1983] “Nonlinear free surface effects: Experiments and theory,” Report No. 83–19. Department of Ocean Engineering, MIT.
- Grilli, S. T. & Watts, P. [1999] “Modeling of waves generated by a moving submerged body. Applications to underwater landslides,” *Journal of Engineering Analysis with Boundary Elements* **23**, 645–656.
- Grilli, S. T. & Watts, P. [2005] “Tsunami generation by submarine mass failure. I: modeling, experimental validation, and sensitivity analyses,” *Journal of Waterways, Port, Coastal, and Ocean Engineering* 283–297 (November/December).
- Gotoh, H., Shibihara, T. & Sakai, T. [2001] “Sub-particle-scale model for the MPS method — Lagrangian flow model for hydraulic engineering,” *Computational Fluid Dynamics Journal* **9**(4), 339–347.
- Heinrich, P. [1992] “Nonlinear water waves generated by submarine and aerial landslides,” *Journal of Waterways, Port, Coastal, and Ocean Engineering* **118**(3), 249–266.
- Hui, S. [2007] “A Boundary Element Method Applied to Strongly Nonlinear Wave-Body Interaction Problems, PhD Thesis, Norwegian University of Science and Technology.
- Jiang, L. & LeBlond, P. H. [1992] “The coupling of a submarine slide and the surface waves which it generates,” *Journal of Geophysical Research* **97**(C8, 12), 731–744.
- Khayyer, A., Gotoh, H. & Shao, S. D. [2008] “Corrected incompressible SPH method for accurate water-surface tracking in breaking waves,” *Coastal Engineering* **55**(3), 236–250.
- Khayyer, A. & Gotoh, H. [2008] “Development of CMPS method for accurate water-surface tracking in breaking waves,” *Coastal Engineering Journal* **50**(2), 179–207.

- Lee, E.-S., Moulinec, C., Xu, R., Violeau, D., Laurence, D. & Stansby, P. [2008] "Comparisons of weakly compressible and truly incompressible algorithms for the SPH mesh free particle method," *Journal of Computational Physics*, S0021-9991(08)00315-X.
- Lo, E. Y. M. & Shao, S. [2002] "Simulation of near-shore solitary wave mechanics by an incompressible SPH method," *Applied Ocean Research* **24**, 275–286.
- Lucy, L. B. [1977] "A numerical approach to the testing of the fission hypothesis," *Astron. J.* **82**, 1013–1024.
- Monaghan, J. J. [1989] "On the problem of penetration in particle methods," *Journal Computational Physics* **82**, 1–15.
- Monaghan, J. J. [1992] "Smoothed particle hydrodynamics," *Annu. Rev. Astron. Astrophys.* **30**, 543–574.
- Monaghan, J. J. [1994] "Simulating free surface flows with SPH," *Journal Computational Physics* **110**, 399–406.
- Monaghan, J. J. & Kos, A. [1999] "Solitary waves on a Cretan beach," *Journal of Waterway, Port, Coastal and Ocean Engineering* **125**(3), 145–154.
- Monaghan, J. J. & Kos, A. [2000] "Scott Russell's wave generator," *Physics of Fluids* **12**, 622–630.
- Morris, J. P., Fox, P. J. & Shu, Y. [1997] "Modeling lower Reynolds number incompressible flows using SPH," *Journal Computational Physics* **136**, 214–226.
- Oger, G., Doring, M., Alessandrini, B. & Ferrant, P. [2006] "Two-dimensional SPH simulations of wedge water entries," *Journal of Computational Physics* **213**(2), 803–822.
- Rzadkiewicz, S., Mariotti, C. & Heinrich, P. [1997] "Numerical simulation of submarine landslides and their hydraulic effects," *Journal of Waterway, Port, Coastal, and Ocean Engineering* **123**(4), 149–157.
- Shao, S. D. & Lo, E. Y. M. [2003] "Incompressible SPH method for simulating Newtonian and non-Newtonian flows with a free surface," *Adv. Water Res.* **26**(7), 787–800.
- SPHysics user guide, version 1.0.002, [2007].
- Sun, H. & Faltinsen, O. M. [2006] "Water impact of horizontal circular cylinders and cylindrical shells," *Applied Ocean Research* **28**(5), 299–311.